

AGING

Cellular survivorship bias as a mechanistic driver of muscle stem cell aging

Jengmin Kang^{1,2,3,†,‡}, Daniel I. Benjamin^{1,2,3,†}, Qiqi Guo^{2,3},
Chauncey Evangelista^{2,3}, Soochi Kim^{1,2,3,§}, Marina Arjona¹,
Pieter Both^{1,4}, Mingyu Chung^{1,2,3}, Ananya K. Krishnan¹,
Gurkamal Dhaliwal¹, Richard Lam¹, Thomas A. Rando^{1,2,3,*}

Aging is characterized by a decline in the ability of tissue repair and regeneration after injury. In skeletal muscle, this decline is largely driven by impaired function of muscle stem cells (MuSCs) to efficiently contribute to muscle regeneration. We uncovered a cause of this aging-associated dysfunction: a cellular survivorship bias that prioritizes stem cell persistence at the expense of functionality. With age, MuSCs increased expression of a tumor suppressor, N-myc down-regulated gene 1 (NDRG1), which, by suppressing the mammalian target of rapamycin (mTOR) pathway, increased their long-term survival potential but at the cost of their ability to promptly activate and contribute to muscle regeneration. This delayed muscle regeneration with age may result from a trade-off that favors long-term stem cell survival over immediate regenerative capacity.

One of the most well-characterized phenotypes of muscle stem cell (MuSC) aging is the slowed rate at which aged MuSCs activate from quiescence and enter the cell cycle (1–4). This slowing directly contributes to the impaired rate at which aged muscle regenerates after injury (1, 2, 5, 6). Indeed, transcriptomic analysis of young and old MuSCs shows that cell cycle and proliferation pathways are among the most altered pathways with age (3, 7). However, the direct mechanistic link between aging and slowed MuSC activation remains incompletely understood.

The tumor suppressor NDRG1 is up-regulated in aged MuSCs

To identify genetic changes that might be responsible for the declining rate of MuSC activation with age, we analyzed the transcriptomes of young and old mouse MuSCs (7). Principal components analysis (PCA) of the RNA sequencing (RNA-seq) data revealed a clear separation between young and old MuSCs, indicating age-associated global transcriptional differences (Fig. 1A). The expression of *N-myc down-regulated gene 1* (*NdrG1*) showed the largest change among growth factor signaling and cell cycle-related genes with age, increasing by 3.5-fold in aged MuSCs (Fig. 1, B and C, and fig. S1A). *NDRG1* acts as a tumor suppressor gene in multiple cell types by blunting numerous growth factor signaling pathways (8–10). Immunofluorescence staining of isolated myofibers from hindlimb muscles and protein immunoblot analysis of isolated MuSCs confirmed the increased accumulation of NDRG1 protein in aged MuSCs (Fig. 1D and fig. S1, B and C).

¹Department of Neurology and Neurological Sciences, Stanford University School of Medicine, Stanford, CA, USA. ²Broad Stem Cell Research Center, University of California Los Angeles, Los Angeles, CA, USA. ³Department of Neurology, University of California Los Angeles, Los Angeles, CA, USA. ⁴Stem Cell Biology and Regenerative Medicine Graduate Program, Stanford University School of Medicine, Stanford, CA, USA. *Corresponding author. Email: trando@mednet.ucla.edu †Present address: Department of Chemistry, Sungkyunkwan University, Suwon, Republic of Korea. ‡Present address: Department of Biotechnology and Bioinformatics, Korea University, Sejong, Republic of Korea. †These authors contributed equally to this work.

NDRG1 gene ablation in aged MuSCs results in enhanced MuSC activation and an improved rate of muscle regeneration

We surmised that the increased abundance of NDRG1 with age might explain the decreased rate of cell cycle entry of aged MuSCs (8–10). To test this, we generated mice with a MuSC-specific conditional deletion of NDRG1 (*Paax7^{Cre}ER/+;NDRG1^{fl/fl};ROSA^{eYFP/+}*, hereafter referred to as NDRG1^{CKO} mice) to ablate NDRG1 after tamoxifen (TMX) injection (fig. S2A). Loss of NDRG1 was confirmed by protein immunoblot analysis of isolated MuSCs and immunofluorescence staining of isolated myofibers (Fig. 2, A and B). To probe NDRG1 function during aging, NDRG1^{CKO} mice were aged to ~20 months and then treated with TMX. Two weeks later, MuSCs were isolated from hindlimb muscles of wild-type (WT) and NDRG1^{CKO} mice (Fig. 2C). Aged NDRG1^{CKO} MuSCs exhibited a significant increase in the rates of S phase entry and mitochondrial accumulation during activation compared with controls, achieving amounts similar to those of young MuSCs (Fig. 2, D and E). To assess the role of NDRG1 ablation in promoting MuSC activation in vivo, EdU was administered to ~20-month-old NDRG1^{CKO} and WT mice after muscle injury. Three days later, activated MuSCs were isolated (Fig. 2F). Consistent with our ex vivo result, MuSCs from old NDRG1^{CKO} mice displayed an increased rate of in vivo activation, similar in magnitude to that of young MuSCs (Fig. 2G).

We tested whether the slowed rate of regeneration characteristic of aged muscle might be driven by increased NDRG1 expression in aged MuSCs. We injured the tibialis anterior muscles of both aged WT and NDRG1^{CKO} mice and measured the extent of regeneration 7 days later (Fig. 2F). The rate of muscle regeneration was increased in NDRG1^{CKO} mice (Fig. 2H and fig. S2B). By contrast, muscle regeneration in young NDRG1^{CKO} mice was not significantly altered compared with age-matched controls (fig. S2, C and D). Thus, increased NDRG1 expression in old MuSCs mediates the slowed rate of MuSC activation and muscle regeneration of aged muscle.

NDRG1 ablation in aged MuSCs results in impaired cell survival and defective regeneration after sequential injuries

Another phenotypic hallmark of aged MuSCs is defective cell survival and resilience (1, 5, 7). Given that aged NDRG1^{CKO} MuSCs appeared rejuvenated with respect to their activation rate, we tested whether NDRG1 ablation affected survival of aged MuSCs and indeed found impaired survival compared with controls (Fig. 3A). Likewise, aged NDRG1^{CKO} mice displayed a reduction in the number of quiescent MuSCs [confirmed by calcitonin receptor (CalcR) staining (11)] 21 days after muscle injury (Fig. 3B and fig. S3A). As defective MuSC survival after injury can lead to impaired muscle regeneration in response to a subsequent injury (1), we induced two sequential injuries in the muscles of aged NDRG1^{CKO} and WT mice (Fig. 3C). Histological analysis revealed that NDRG1^{CKO} mice displayed an impairment in muscle regeneration after the second injury (Fig. 3D), likely owing to the reduced MuSC pool available for regeneration and in spite of the enhanced regenerative potential of NDRG1^{CKO} MuSCs. We observed a further reduction in quiescent MuSCs 21 days after a second injury in the NDRG1^{CKO} mice (Fig. 3E).

Thus, NDRG1 may mediate a critical phenotypic trade-off in aged MuSCs. Whereas NDRG1 expression blunts the ability of MuSCs to activate promptly and regenerate muscle efficiently, it also promotes MuSC survival, suggesting a trade-off between activation rate and resilience (12). To test whether accumulation of NDRG1 with age is a consequence of a survivorship bias that privileges cell resilience over cell function, we ablated NDRG1 in the MuSCs of young mice and subsequently aged the mice for a period of 18 to 20 months (Fig. 3F). Indeed, aged NDRG1^{CKO} mice displayed a decrease in the total MuSC pool compared with that of their age-matched WT counterparts (Fig. 3G and fig. S3, B and C). Aged NDRG1^{CKO} mice also showed significantly delayed muscle regeneration (Fig. 3H), likely as a consequence of the reduction in the number of surviving MuSCs. Despite the selection for

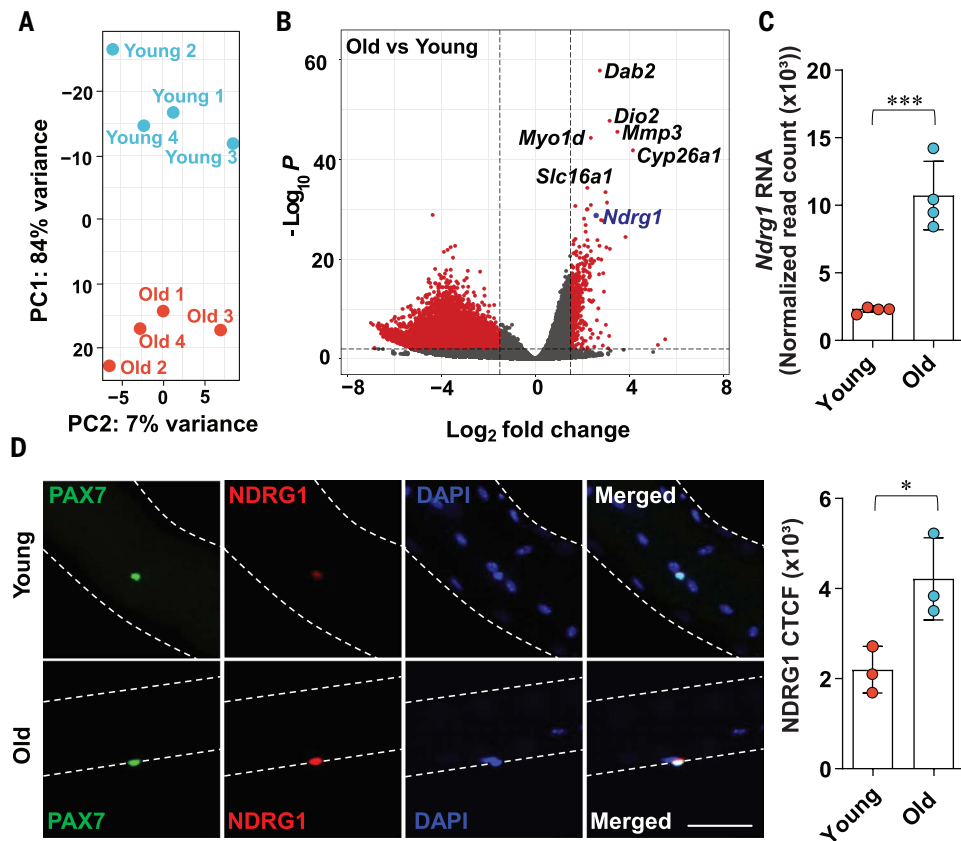


Fig. 1. Increased abundance of NDRG1 transcripts and protein in aged MuSCs. (A) PCA plot of RNA-seq data from freshly isolated MuSCs from young (3-month-old) and old (22-month-old) mice. (B) Volcano plots of differentially expressed genes. Dashed lines indicate fold change ($\log_2FC > 1.5$) and P value cutoffs ($P_{adj} < 0.05$). (C) Normalized DESeq read counts of *NdrG1*. (D) (Left) Representative immunofluorescence images of extensor digitorum longus (EDL) single myofibers. PAX7, paired box protein 7; DAPI, 4',6-diamidino-2-phenylindole (scale bar, 50 μ m). (Right) Corrected total cell fluorescence (CTCF) for NDRG1. P values were calculated with a two-sided unpaired Student's t test. Data are shown as mean \pm SD in (C) and (D); * $P < 0.05$; *** $P < 0.001$.

resilience with age, old MuSCs are still less resilient than their young counterparts. Although NDRG1 enhances the resilience of old MuSCs, there still exist a multitude of other factors that combine to make old MuSCs less resilient than young MuSCs (5, 7, 12).

This survivorship bias theory of cellular aging begs a crucial evolutionary question: If NDRG1 expression confers a cellular survival benefit that is selected for with age, why would NDRG1 not simply be removed from the gene pool if it did not confer benefit during youth, when the forces of natural selection are strongest? To address this question, we ablated NDRG1 in young mice and measured regeneration after either a single injury or consecutive injuries (fig. S3D). Although, as previously noted (fig. S2D), removal of NDRG1 had no significant effect on the regeneration of young muscle after a single injury, this was associated with a decline in the total number of MuSCs (fig. S3, E and F). In response to a subsequent injury, we observed an even greater decline in total MuSCs and now a regenerative impairment (fig. S3, G and H). These results support a trade-off model in which low NDRG1 expression in young stem cells enables rapid regeneration while maintaining a baseline level of resilience, which is sufficient for survival in young animals but inadequate for survival in the harsher environment of aged tissue.

To test the idea that increased NDRG1 in young MuSCs would be detrimental, we isolated a population of young MuSCs that had the highest NDRG1 amounts and compared them using functional assays

with MuSCs with the lowest NDRG1 expression from the same mice (fig. S4, A and B). Young NDRG1^{high} MuSCs exhibited reduced activation rates compared with their NDRG1^{low} counterparts (fig. S4C). We then transplanted NDRG1^{high} and NDRG1^{low} MuSCs and monitored the cells using bioluminescence imaging. Bioluminescence intensities in muscles transplanted with NDRG1^{high} MuSCs were significantly lower (fig. S4D), which is consistent with a slower rate of activation. As an independent test of the consequences of increased NDRG1 in young MuSCs, we overexpressed NDRG1 in freshly isolated MuSCs from young mice (fig. S4E). Overexpression of NDRG1 resulted in reduced activation rates (fig. S4F). Likewise, muscles transplanted with NDRG1-overexpressing cells showed significantly lower signals than did control cells (fig. S4G).

Although we observed no significant change in MuSC survival by NDRG1 overexpression under control conditions, NDRG1-expressing MuSCs showed improved survival under conditions of oxidative stress (fig. S4, H and I). Thus, overexpression of NDRG1 in young MuSCs slows the rate of their activation, but as with aged MuSCs, this is accompanied by increased resilience.

The phenotypic consequences of NDRG1 accumulation in aged MuSCs are mediated by repression of the PI3K-AKT-mTOR pathway

We sought to determine the molecular mechanism by which NDRG1 elicited effects in old MuSCs. We therefore performed RNA-seq of MuSCs from aged WT and NDRG1^{CKO} mice. PCA showed distinct clustering of WT and NDRG1^{CKO} MuSCs, and volcano plot analysis revealed numerous differentially expressed genes (fig. S5, A and B). Gene set enrichment analysis revealed increased abundance of mRNAs encoding proteins in the phosphatidylinositol 3-kinase (PI3K)-AKT-mTOR pathway upon NDRG1 ablation (Fig. 4, A and B). We confirmed increased activation of this pathway after NDRG1 ablation by protein immunoblotting (Fig. 4, C to E). Analysis of our RNA-seq data revealed up-regulation of several genes in the PI3K-Akt-mTOR pathway (*PIK3CA*, *AKT1*, *PTEN*, and *CXCR4*) in NDRG1-ablated MuSCs (fig. S5C). We also found that phosphorylation of S6, a downstream target of the mTOR pathway, was increased in NDRG1^{CKO} MuSCs and was reduced upon treatment with the mTOR inhibitor rapamycin (fig. S5D). Given the role of the mTOR pathway in promoting cell cycle progression (13), we tested whether the enhanced activation rate of aged NDRG1^{CKO} MuSCs is mediated by the mTOR pathway. Inhibition of mTOR with rapamycin blunted the enhanced rate of S phase entry in NDRG1^{CKO} MuSCs (Fig. 4F).

Activation of mTOR in quiescent MuSCs results in a primed state termed G_{Alert} (14), which is characterized by accelerated activation and mediates enhanced muscle regeneration. On the basis of increased mTOR signaling in NDRG1^{CKO} MuSCs, we tested whether they also exist in this alerted state. Two hallmarks of MuSCs in G_{Alert} are an increased propensity to spontaneously exit quiescence and an increased size. Indeed, old NDRG1^{CKO} MuSCs displayed these phenotypes, whereas

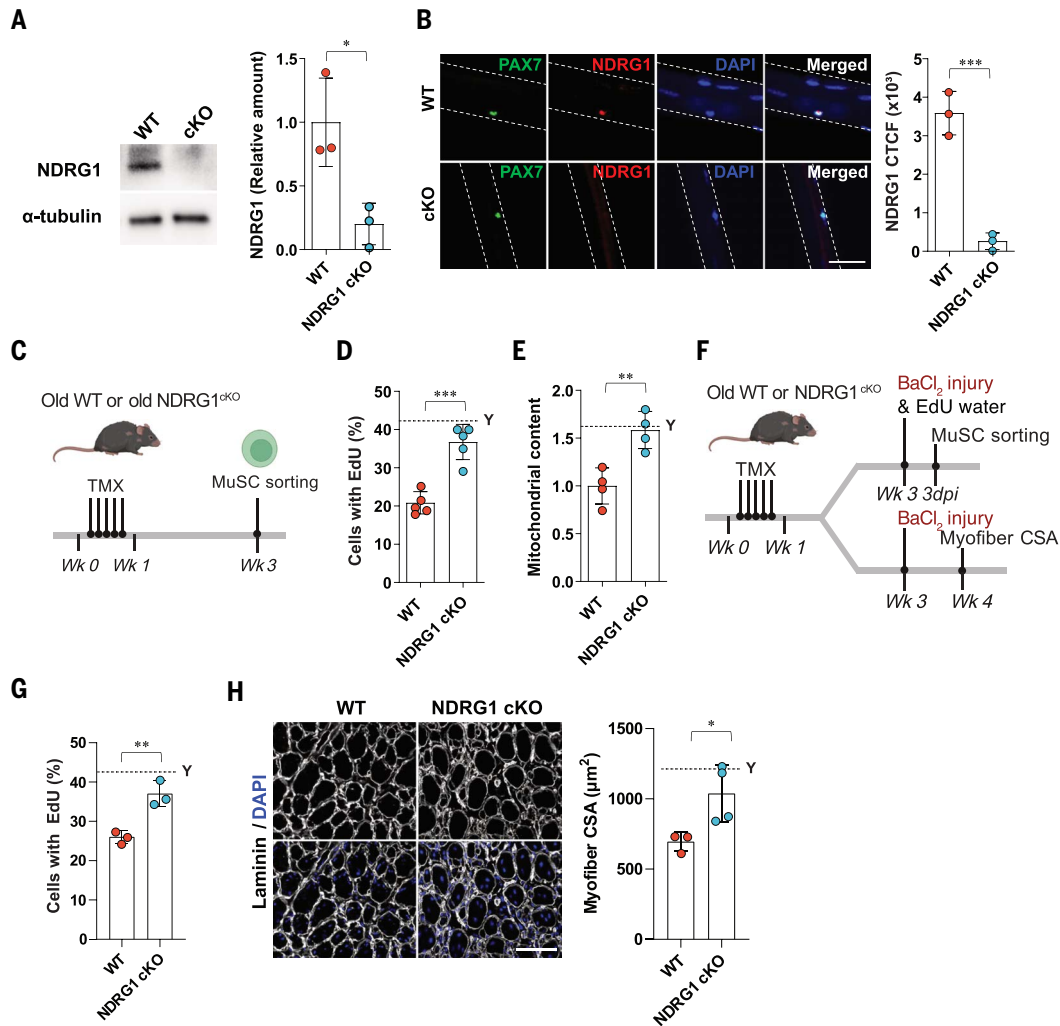


Fig. 2. Enhanced MuSC activation and improved muscle regeneration after NDRG1 ablation in aged MuSCs. (A) (Left) Representative immunoblots of yellow fluorescent protein-positive (YFP⁺) MuSCs isolated from WT and NDRG1^{cKO} mice. (Right) Band intensities of NDRG1 were normalized to those of α -tubulin ($n = 3$). (B) (Left) Representative immunofluorescence images of EDL single myofibers (scale bar, 50 μ m). (Right) CTCF for NDRG1 measured in YFP⁺ WT and NDRG1^{cKO} MuSCs. (C) Schematic for TMX injection and YFP⁺ MuSC isolation from old WT and NDRG1^{cKO} mice. (D) 5-ethynyl-2'-deoxyuridine (EdU) incorporation in old YFP⁺ MuSCs. MuSCs were maintained in culture for 40 hours in the continuous presence of EdU. The dashed line indicates mean value of EdU incorporation in young MuSCs ($n = 5$). (E) Relative mitochondrial content measured in old YFP⁺ MuSCs. The dashed line indicates mean value of mitochondrial content in young MuSCs ($n = 4$). (F) Schematic for TMX injection, BaCl₂ injury, and in vivo EdU administration related to (G) and (H). CSA, cross-sectional area; dpi, days post infection; Wk, week. (G) In vivo EdU incorporation in old YFP⁺ MuSCs. EdU was administered for 3 days after muscle injury. The dashed line indicates mean value of in vivo EdU incorporation in young MuSCs ($n = 3$). (H) (Left) Representative immunostaining of regenerating muscle fibers for WT and NDRG1^{cKO} mice 7 days after injury (scale bar, 100 μ m). (Right) Quantification of the mean CSAs of centrally nucleated myofibers in muscle sections ($n = 3$ for WT, $n = 4$ for NDRG1^{cKO}). The dashed line indicates mean CSA in young mice 7 days after injury ($n = 3$). P values were calculated with a two-sided unpaired Student's t test. Data are shown as mean \pm SD in (A), (B), (D), (E), (G), and (H); * $P < 0.05$, ** $P < 0.01$, *** $P < 0.001$.

young NDRG1^{cKO} MuSCs did not (Fig. 4, G to I, and fig. S5, E and F). Both of these G_{Alert} phenotypes were abrogated by rapamycin treatment (Fig. 4, J to L), further highlighting the similarities between NDRG1^{cKO} G_{Alert} MuSCs (14). Likewise, the ablation of NDRG1 in MuSCs did not result in any evidence of muscle injury that might secondarily lead to MuSC activation (fig. S5, G to K).

MuSCs in G_{Alert} exhibit an mTOR-dependent deficit in survival and in long-term persistence (15), similar to that of NDRG1^{cKO} MuSCs. Treating old NDRG1^{cKO} mice with rapamycin partially rescued the survival impairments associated with NDRG1 ablation (Fig. 4M). Additionally, rapamycin treatment blunted the enhanced rate of S phase entry and mitochondrial accumulation characteristic of NDRG1-ablated MuSCs (fig. S6, A and B). Rapamycin treatment also rescued the regenerative impairments of NDRG1^{cKO} mice after sequential injuries

(fig. S6, C and D). Thus, the accumulation of NDRG1 with age suppresses mTOR signaling in MuSCs, rendering the cells less prone to activate but more resilient. These conditions are in direct contrast to the G_{Alert} state, in which MuSCs have increased mTOR signaling and are thus more poised to activate but have reduced resilience (14, 15).

These findings support the conclusion that the accumulation of NDRG1, and the associated suppression of mTOR signaling, may be the result of a survivorship bias that eliminates MuSCs with low NDRG1 expression that are less resilient, leaving MuSCs that have higher NDRG1 expression but are less able to support rapid regeneration. MuSCs that do not accumulate NDRG1 during aging are highly prone to being depleted from the MuSC pool over time. This view of aging is distinct from the antagonistic pleiotropy theory, which proposes that aging-associated phenotypic dysfunction is a consequence of specific genes whose expression

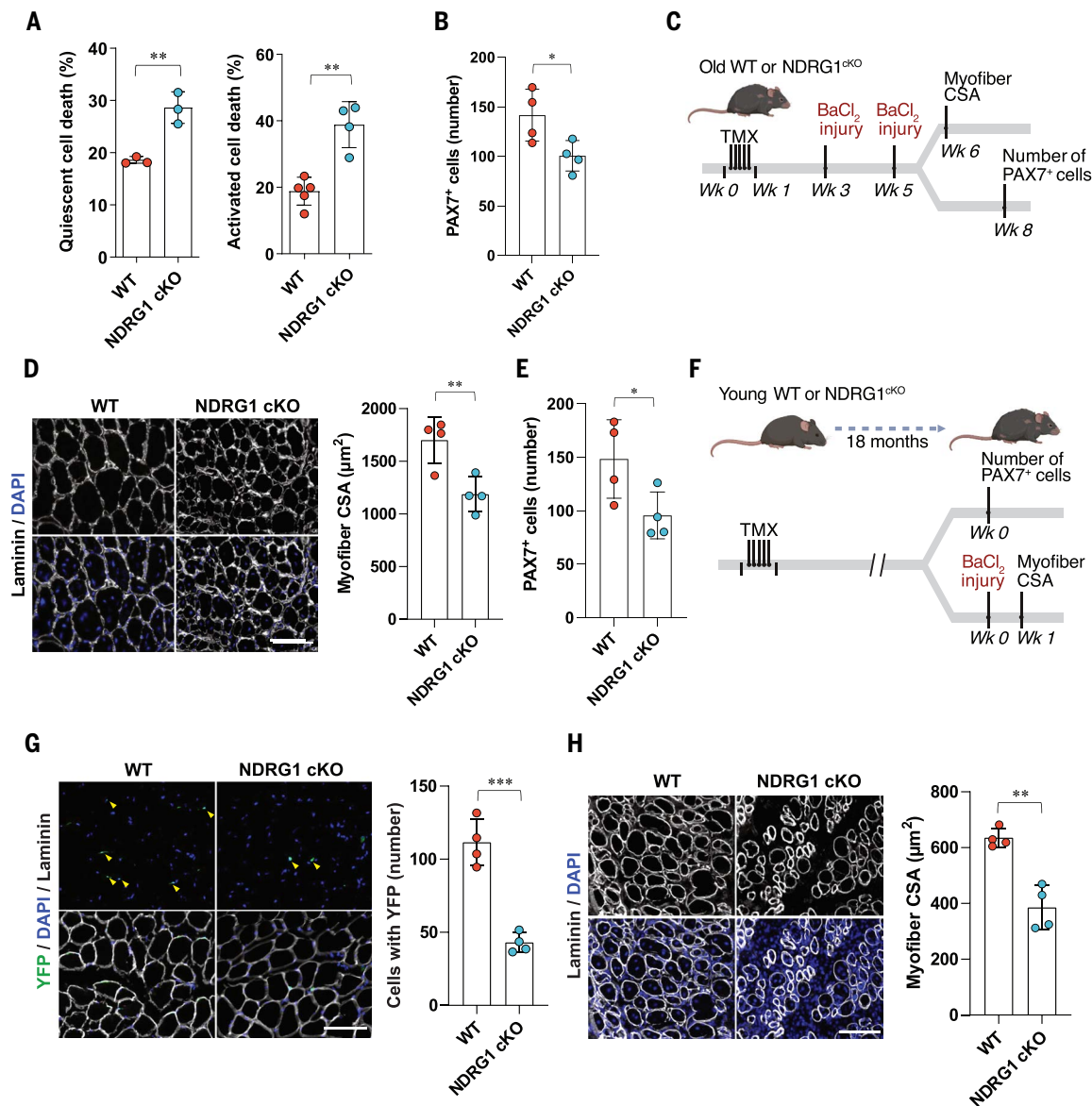


Fig. 3. Impaired cell survival and defective regeneration of aged muscle after sequential injuries in MuSCs lacking NDRG1. (A) (Left) Dead cells were quantified immediately upon isolation of old YFP⁺ MuSCs ($n = 3$). (Right) Quantification of dead cells during activation. Dead cells were counted 40 hours after plating ($n = 5$ for WT, $n = 4$ for NDRG1^{cKO}). (B) Quantification of number of PAX7⁺ MuSCs per each tissue section 21 days after injury ($n = 4$). (C) Schematic for TMX injection and repetitive BaCl₂ injuries related to (D) and (E). (D) (Left) Representative immunostaining of regenerating muscle fibers 7 days after the second injury (scale bar, 100 μ m). (Right) Quantification of the mean CSA of centrally nucleated myofibers in muscle sections ($n = 4$). (E) Quantification of number of PAX7⁺ MuSCs per each tissue section 21 days after the second injury ($n = 4$). (F) Schematic for TMX injection and BaCl₂ injury related to (G) and (H). (G) (Left) Representative tissue immunostaining images of muscle sections (scale bar, 100 μ m). (Right) Quantification of the number of YFP⁺ MuSCs per tissue section ($n = 4$). (H) (Left) Representative immunostaining of regenerating muscle fibers (scale bar, 100 μ m). (Right) Quantification of the mean CSAs of centrally nucleated myofibers in muscle sections ($n = 4$). P values were calculated with a two-sided unpaired Student's t test. Data are shown as mean \pm SD in (A) to (C), (E), (F), (H), and (I); * $P < 0.05$, ** $P < 0.01$, *** $P < 0.001$.

confers benefits to organisms during youth but detriments to organisms with age (16)—based on the idea that natural selection strongly favors early-life benefits even when they come at the cost of late-life harm. By contrast, *NDRG1* is an example of a gene whose increased expression would be largely detrimental during youth because of the impaired regenerative response but emerges prominently with age as a result of a strong survivorship bias conferred to cells with high levels of NDRG1.

Thus, our work not only reveals an unexpected cause of impaired tissue regeneration with age but also leads us to propose a conceptual framework of organismal aging in which cell-specific survivorship bias,

rather than antagonistic pleiotropy, underlies functional decline with age. Additionally, our findings highlight the fact that molecular changes associated with cellular aging may be positive compensatory responses as opposed to drivers of age-related decline. In this case, delayed activation or reduced regenerative capacity might be interpreted as purely detrimental consequences of aging. However, the trade-off for such detrimental changes, namely enhanced resilience, may avoid a much worse outcome—the depletion of the stem cell pool and even less-effective tissue maintenance and regeneration. Thus, aging-associated change in gene expression, although costly in terms of cellular function, may in fact support cellular survival and tissue integrity into old age.

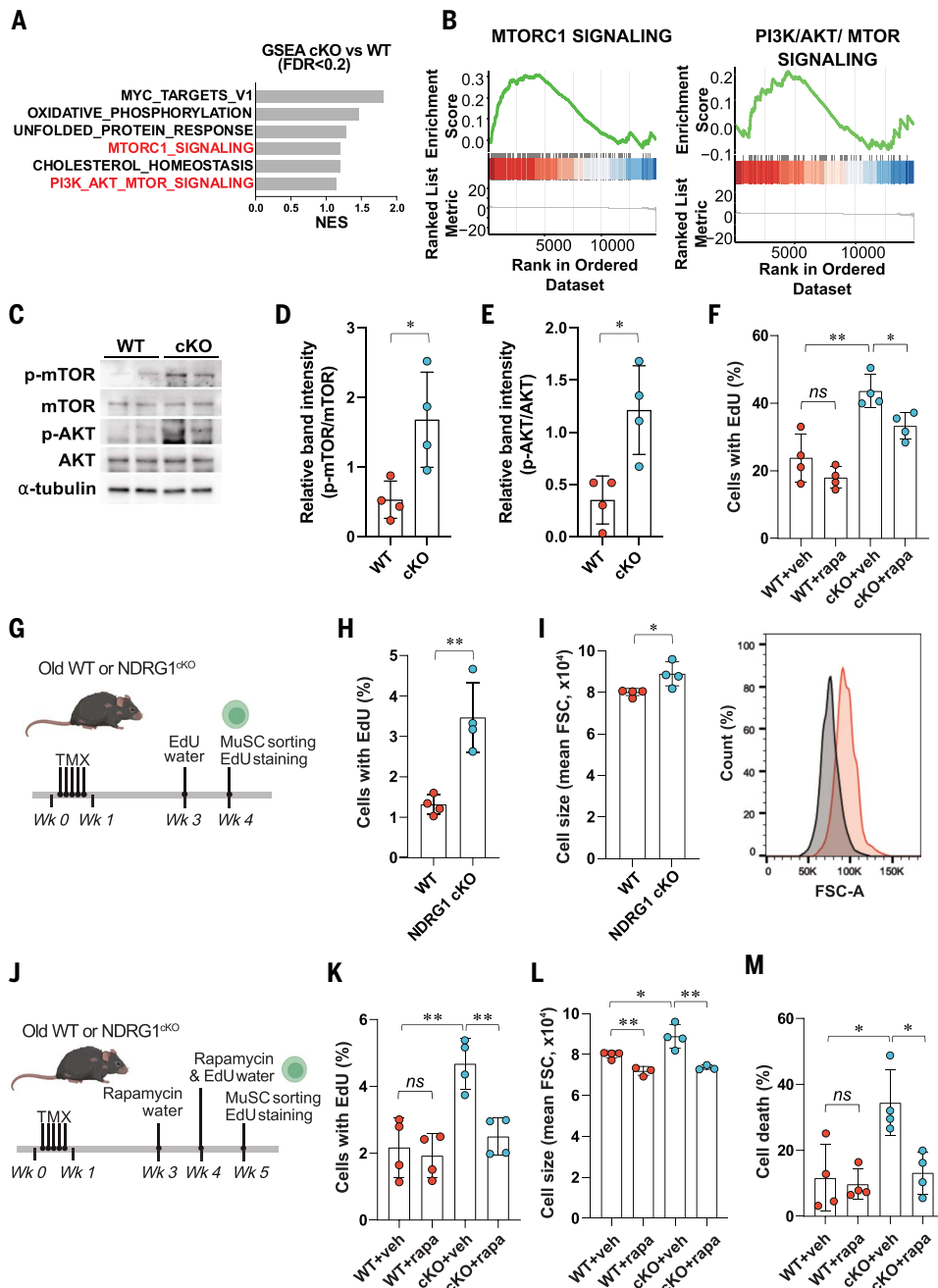


Fig. 4. Assessments of phenotypic consequences of increased NDRG1 in aged MuSCs downstream repression of the PI3K-AKT-mTOR pathway. (A) Gene set enrichment analysis (GSEA) of hallmark gene sets enriched in differentially expressed genes in old MuSCs. FDR, false discovery rate; NES, normalized enrichment score. (B) GSEA signature plots. (C) Representative immunoblots of MuSCs isolated from old WT and NDRG1^{CKO} mice. (D and E) From replicate studies as shown in (C), band intensities of p-mTOR and p-AKT were normalized to those of total mTOR and AKT, respectively ($n = 4$). (F) Freshly isolated old WT and NDRG1^{CKO} MuSCs were treated with 100 nM of rapamycin (rap) for 48 hours. EdU incorporation in the MuSCs was quantified after 40 hours culture in the continuous presence of EdU ($n = 4$). veh, vehicle. (G) Schematic of TMX injection and in vivo EdU treatment. (H) In vivo EdU incorporation in YFP⁺ MuSCs isolated from each group of mice treated as described in (G) ($n = 4$). (I) (Left) YFP⁺ MuSC size was measured as forward angle light scatter (FSC) with flow cytometry ($n = 4$). (Right) Representative fluorescence-activated cell sorting plot. (J) Schematic of tamoxifen injection and rapamycin and EdU treatments related to (K) and (L). (K) Spontaneous cell cycle entry in the absence of injury measured by in vivo EdU incorporation in freshly isolated MuSCs ($n = 4$). (L) Quantification of cell size by FSC ($n = 4$). (M) Quantification of dead YFP⁺ MuSCs upon isolation ($n = 4$). P values were calculated with a two-sided unpaired Student's t test. Data are shown as mean \pm SD in (D) to (F), (H), (I), and (K) to (M); * $P < 0.05$, ** $P < 0.01$; ns, not significant.

REFERENCES AND NOTES

- L. Liu *et al.*, *Cell Stem Cell* **23**, 544–556.e4 (2018).
- I. M. Conboy *et al.*, *Nature* **433**, 760–764 (2005).
- J. O. Brett *et al.*, *Nat. Metab.* **2**, 307–317 (2020).
- S. C. Schuler *et al.*, *Cell Rep.* **35**, 109223 (2021).
- J. Kang *et al.*, *Nat. Metab.* **6**, 153–168 (2024).
- H. M. Blau, B. D. Cosgrove, A. T. Ho, *Nat. Med.* **21**, 854–862 (2015).
- D. I. Benjamin *et al.*, *Cell Metab.* **35**, 472–486.e6 (2023).
- K. C. Park *et al.*, *Biochim. Biophys. Acta Mol. Basis Dis.* **1864**, 2644–2663 (2018).
- S. K. Kachhap *et al.*, *PLOS ONE* **2**, e844 (2007).
- Y. Nakahara *et al.*, *Brain Sci.* **12**, 473 (2022).
- L. Zhang *et al.*, *Cell Rep.* **29**, 2154–2163.e5 (2019).
- D. I. Benjamin *et al.*, *Cell Metab.* **34**, 902–918.e6 (2022).
- M. Laplante, D. M. Sabatini, *Cell* **149**, 274–293 (2012).
- J. T. Rodgers *et al.*, *Nature* **510**, 393–396 (2014).
- S. Haller *et al.*, *Cell Stem Cell* **21**, 806–818.e5 (2017).
- G. C. Williams, *Evolution* **11**, 398–411 (1957).

ACKNOWLEDGMENTS

Funding: This work was supported by the National Research Foundation of Korea RS-2025-00515310 (J.K.); NIH grants AG36695, AG68667, and AG82764 (T.A.R.); the NOMIS Foundation (T.A.R.); the Milky Way Research Foundation (T.A.R.); and the Evolution Foundation (T.A.R.). **Author contributions:** Conceptualization: D.I.B., T.A.R.; Investigation: J.K., D.I.B., Q.G., C.E., S.K., M.A., P.B., G.D., R.L., A.K., M.C.; Supervision: T.A.R.; Writing – original draft: J.K., D.I.B.; Writing – review & editing: J.K., D.I.B., T.A.R. **Competing interests:** The authors declare that they have no competing interests. **Data, code, and materials availability:** RNA-seq data have been deposited in NCBI's Gene Expression Omnibus (GEO) with accession no. GSE275358. All data are available in the main text or the supplementary materials. **License information:** Copyright © 2026 the authors, some rights reserved; exclusive licensee American Association for the Advancement of Science. No claim to original US government works. <https://www.science.org/about/science-licenses-journal-article-reuse>

SUPPLEMENTARY MATERIALS

[science.org/doi/10.1126/science.ads9175](https://www.science.org/doi/10.1126/science.ads9175)
Materials and Methods; Figs. S1 to S6;
References (17, 18); MDAR Reproducibility Checklist
Submitted 5 September 2024; resubmitted 9 May 2025; accepted 20 October 2025

10.1126/science.ads9175



Cellular survivorship bias as a mechanistic driver of muscle stem cell aging

Jengmin Kang, Daniel I. Benjamin, Qiqi Guo, Chauncey Evangelista, Soochi Kim, Marina Arjona, Pieter Both, Mingyu Chung, Ananya K. Krishnan, Gurkamal Dhaliwal, Richard Lam, and Thomas A. Rando

Science **391** (6784), . DOI: 10.1126/science.ads9175

Editor's summary

Muscle stem cells lose their regenerative capacities with age, and Kang *et al.* have demonstrated a role of *NDRG1* (*N-myc downregulated gene 1*), a tumor suppressor gene, in this process. Expression of *NDRG1* was increased in muscle cells from old mice, and genetic depletion of the gene enhanced muscle regeneration (see the Perspective by von Maltzahn). However, there was a trade-off, and loss of *NDRG1* wasn't wholly beneficial. Cell survival and regeneration were reduced after multiple injuries. Thus, the characteristics of aged muscle cells may reflect not so much a general decline in function as selection of those cells with high *NDRG1* expression. This trade-off may allow for resilience and survival for aged muscles but with delayed activation and decreased regenerative capacity. —L. Bryan Ray

View the article online

<https://www.science.org/doi/10.1126/science.ads9175>

Permissions

<https://www.science.org/help/reprints-and-permissions>

Use of this article is subject to the [Terms of service](#)

Science (ISSN 1095-9203) is published by the American Association for the Advancement of Science. 1200 New York Avenue NW, Washington, DC 20005. The title *Science* is a registered trademark of AAAS.

Copyright © 2026 The Authors, some rights reserved; exclusive licensee American Association for the Advancement of Science. No claim to original U.S. Government Works